Synthesis of nordihydroguaiaretic acid derivatives and their bioactivities on S. pombe and K562 cell lines

ARTICLE *in* EUROPEAN JOURNAL OF MEDICINAL CHEMISTRY · FEBRUARY 2013

Impact Factor: 3.45 · DOI: 10.1016/j.ejmech.2013.01.028 · Source: PubMed

European Journal of Medicinal Chemistry 62 (2013) 605–613

Contents lists available at SciVerse ScienceDirect

European Journal of Medicinal Chemistry

journal homepage: http://www.elsevier.com/locate/ejmech

Original article

Synthesis of nordihydroguaiaretic acid derivatives and their bioactivities on *S. pombe* and *K562* cell lines

Xu Li [a], Jian-Hong Jiang [a], Qingqi Chen [b,**], Sheng-Xiong Xiao [a], Chuan-Hua Li [a], Hui-Wen Gu [c,***], Hui Zhang [a], Ji-Lin Hu [a], Fei-Hong Yao [a], Qiang-Guo Li [a,*]

[a] *Hunan Provincial Key Laboratory of Xiangnan Rare-Precious Metals Compounds and Applications, Department of Chemistry and Life Science, Xiangnan University, Chenzhou 423000, Hunan Province, PR China*
[b] *MedKoo Biosciences, Inc. P O Pox 16222, Chapel Hill, NC 27516-6222, USA*
[c] *State Key Laboratory of Chemo/Biosensing and Chemometrics, College of Chemistry and Chemical Engineering, Hunan University, Changsha 410082, Hunan Province, PR China*

ARTICLE INFO

Article history:
Received 23 October 2012
Received in revised form
14 January 2013
Accepted 22 January 2013
Available online 4 February 2013

Keywords:
Nordihydroguaiaretic acid
NDGA derivatives
Microcalorimetry
Anticancer
S. pombe
K562

ABSTRACT

Nordihydroguaiaretic acid (NDGA) and its synthetic analogues are potentially useful in treating diseases related to cancers, diabetes, viral and bacterial infections, and inflammation. In this paper, we report the optimal synthetic methods and the bioactivity study of terameprocol **2**, NDGA derivative **3**, and its cyclized analogue **4**. The IC_{50} of these three compounds **2**, **3** and **4** on the growth metabolism of *Schizosacchromyces pombe* and *K562* cell lines were determined by microcalorimetry. The preliminary results showed that the compounds **2**, **3** and **4** possessed good inhibition activities on *S. pombe* and *K562* cell lines, and exhibited bidirectional biological effect and Hormesis effect. In particular, terameprocol **2** was found to possess the most potent inhibitory effect on *K562* cell lines.

1. Introduction

During the past century nordihydroguaiaretic acid (NDGA, **1**) (see Fig. 1), one of the naturally occurred lignins, has been an attractive research topic due to its broad range of bioactivities and potential medical applications [1–4] on the cardiovascular, immune and neurological systems, cancer, tissue engineering, etc. NDGA as a drug (generic name: masoprocol, trade name: Actinex®) was approved by Food and Drug Administration (FDA, USA) in September 1992. Actinex® is an antineoplastic drug used to treat skin growths caused by sun exposure, which contains 10% masoprocol or NDGA, is a topical cream product, developed by University of Arizona Cancer Center. However, masoprocol was discontinued in June 1996 due to its low market demand and minor side effects. Terameprocol **2** (see Fig. 1), commonly known as tetra-*O*-methyl-nordihydroguaiaretic acid, EM-1421 and M4N, is a semisynthetic natural product. Remarkably, terameprocol **2**, currently being developed by Erimos Pharmaceuticals, is a promising anticancer agent currently under Phase I/II clinical trials, which is the first NDGA derivative in clinical trials. Although NDGA has been extensively studied during the past decades, NDGA derivatives have been less explored.

Biological microcalorimetry, providing a continuous measurement of heat production, can be employed to directly determine the biological activities of a living system. Heat flux is an expression of overall metabolic flux, and the detection of small changes in heat production to respond to toxic insult will be a sensitive indicator of altered metabolism. Since microcalorimetry is a nondestructive method with high accuracy and automaticity, it is now widely applied in biological research [5] and pharmacological analysis [6].

In this paper we report the optimal synthetic methods and the anticancer activities of DNGA derivative **3** (see Fig. 2), its cyclized analogue **4** (see Fig. 2) and terameprocol **2**. Their bioactivities were determined by microcalorimetry [7–9], cytomorphology, and fluorescence probe method. The results showed that terameprocol **2**, NDGA derivative **3** and its cyclized analogue **4** exhibited good inhibitory activities on the growth metabolism of *Schizosacchromyces pombe* and *K562* cell lines. The values of IC_{50} of

* Corresponding author. Tel./fax: +86 735 2653353.
** Corresponding author. Tel./fax: +1 704 967 0446.
*** Corresponding author. Tel./fax: +86 182 73153402.
E-mail addresses: qqchen@gmail.com (Q. Chen), gruyclewee@hnu.edu.cn (H.-W. Gu), liqiangguo@163.com (Q.-G. Li).

0223-5234/$ – see front matter © 2013 Elsevier Masson SAS. All rights reserved.
http://dx.doi.org/10.1016/j.ejmech.2013.01.028

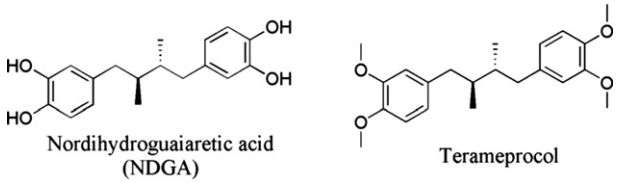

Fig. 1. Structure of NDGA **1** and terameprocol **2**.

terameprocol **2**, NDGA derivative **3** and NDGA derivative **4** on the growth metabolism of *S. pombe* cell lines were found to be 330.0, 290.0 and 350.0 mg L^{-1}, respectively. The values of IC_{50} of terameprocol **2**, NDGA derivative **3** and NDGA derivative **4** on the growth metabolism of *K562* cell lines were found to be 5.87, 8.57 and 11.23 mg L^{-1}, respectively. The inhibitory activity of these three compounds on the growth metabolism of the *S. pombe* has been observed to decrease in the order of NDGA derivative **3** > terameprocol **2** > NDGA derivative **4**. While their inhibitory activity on *K562* cell lines was found to decrease in the order of terameprocol **2** > NDGA derivative **3** > NDGA derivative **4.**

2. Results and discussions

2.1. Chemistry

NGDA derivatives **2**–**4** were synthesized using our developed procedures based on literature reports [10–12], and were outlined as in Fig. 3.

The key step to establish the stereochemistry of terameprocol **2** was the hydrogenation of tetra-substituted furan **4** to give the corresponding *cis*-tetrahydrofuran **9**. The synthesis started with veratrole **5**, which was acylated with propionyl chloride **6** using chloroform as solvent to give a higher yield (94%) of the corresponding ketone **7**. Bromination of compound **7** in refluxing chloroform then gave α-bromo-3,4-dimethoxypropiophenone **8** in 95% yield. Alkylation of **7** in liquid ammonia and sodium amide (produced in situ via adding sodium) at 33 °C with the bromoketone **8** gave racemic diketone **3** in 93%. The synthesis of compound **9** was also reported by Faid et al. [12], who used sodium amide (in situ produced), ferric chloride as catalysts and liquid ammonia as solvent. Cyclodehydration of **9** in 1% HCl–MeOH under reflux to give the corresponding furan compound **4**, followed by hydrogenation created the *cis*-tetrahydrofuran **9**, which was further converted to terameprocol **2** via catalytic hydrogenation as shown in Fig. 3.

After preparing NDGA derivatives **3**, **4** and terameprocol **2**, we next evaluate their bioactivities on *S.pombe* and *K562* cell lines (tumor cell lines) using micocalorimetry. The microcalorimetric study was performed on a 3116-2/3239 TAM Air isothermal calorimeter (Thermometric AB, Sweden).

2.2. Bioactivity

2.2.1. Microcalorimetry

The thermogenic curves (power–time curves) for the growth metabolism of *S. pombe* cells [13] treated by different concentrations of terameprocol **2**, NDGA derivative **3** and NDGA derivative **4** were recorded on the TAM Air microcalorimeter at 32.00 °C, respectively. All microcalorimetric experiments were repeated three times. The results are illustrated in Fig. 4. From Fig. 4, we can find that the thermogenic curves are similar to those of *S.pombe* treated by different concentrations of three compounds.

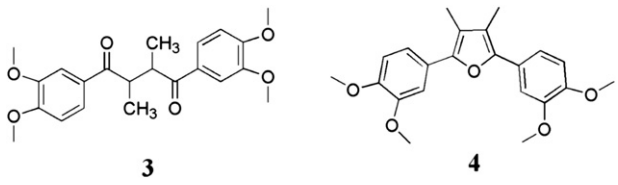

Fig. 2. Structure of NDGA derivative **3** and its cyclized analogue **4**.

2.2.1.1. The growth rate constant (κ) of S. pombe cells. As shown in Fig. 4a, the power–time curve of growth of *S. pombe* cells showed that growth of *S. pombe* cells could be divided into four phases, that is, a lag phase (AB), a log phase (BC), a stationary phase (CD) and a decline phase (DE). During the log phase, the power–time curves obeyed the following equation:

$$n_t = n_0 \exp[k(t - t_0)] \tag{1}$$

where t was the time after the start of exponential growth phase, t_0 was the start time of exponential growth phase, n_t and n_0 were the cell number at time t and t_0, respectively. If the power output of each *S. pombe* cell was one w, then

$$n_t w = n_0 w \exp[k(t - t_0)] \tag{2}$$

If $p_t = n_t w$, $p_0 = n_0 w$, then

$$p_t = p_0 \exp[k(t - t_0)] \tag{3}$$

or

$$\ln p_t = \ln p_0 - kt_0 + kt \tag{4}$$

where P_t was the heat output power of the *S. pombe* cell at time t, and k was the growth rate constant of the *S. pombe* cell at specified conditions, whose size represented growth speed. Using this equation, the growth rate constant k could be calculated and the results are shown in Table 1. It could be seen from Fig. 4 and Table 1 that the compounds **2, 3** and **4** possessed the bidirectional biological effect and Hormesis effect, i.e., these three compounds stimulated the growth of *S. pombe* at low concentration, but inhibited the growth of *S. pombe* at high concentration.

2.2.1.2. Inhibition ratio (I) and half inhibition concentration (IC_{50}). The inhibition ratio of the growth metabolism of *S. pombe* cells treated by drugs was defined as following:

$$I = (k - k_c)/k_0 \times 100\% \tag{5}$$

where k_0 was the control rate constant (without any drug inhibition) of *S. pombe* and k_c was the growth rate constant of *S. pombe* treated by an inhibitor with a concentration of c. The values of (I) are shown in Table 1. When the inhibition ratio was 50%, the drug concentration was called as the half inhibition concentration (IC_{50}). The results showed that terameprocol **2**, NDGA derivative **3** and NDGA derivative **4** possessed significantly inhibitory effect on the growth metabolism of *S. pombe* cell lines. The values of IC_{50} of terameprocol **2**, NDGA derivatives **3**, and NDGA derivatives **4** on the growth metabolism of *S. pombe* cell lines were 330.0, 290.0 and 350.0 mg L^{-1}, respectively. The inhibitory ability of these three compounds above on the growth of the *S. pombe* has been observed to decrease according to the following order: NDGA derivative **3** > terameprocol **2** > NDGA derivative **4**. The NDGA derivative **2, 3** and **4** possessed the bidirectional biological effect and Hormesis effect. In other words, they stimulated the growth of the *S.pombe* at low concentration, but inhibited the growth at high concentration.

The thermogenic curves for the growth metabolism of *K562* cell lines treated by different concentrations of the compounds

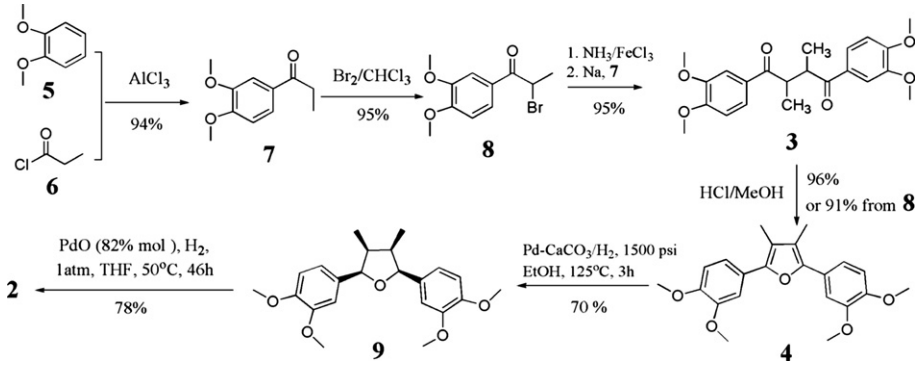

Fig. 3. Synthesis of terameprocol **2** through hydrogenation.

terameprocol **2**, NDGA derivative **3** and NDGA derivative **4** were determined using the TAM Air calorimeter at 37.00 °C, respectively. All microcalorimetric experiments were repeated three times. The results were illustrated in Fig. 5, in which the log phase of thermogenic curves obeyed Eq. (4). Using this equation, the growth rate constant k could be calculated and the results were shown in Table 2. According to Eq. (5), the inhibition ratio (I) of the growth metabolism of *K562* cells treated by the terameprocol **2**, NDGA derivative **3** and NDGA derivative **4** could be calculated and the results were shown in Table 2.

As can be seen from Fig. 5 and Table 2 that the compound terameprocol **2**, NDGA derivative **3** and NDGA derivative **4** possessed the bidirectional biological effect and Hormesis effect, that is, they stimulated the growth of *K562* at low concentration, but inhibited the growth of *K562* at high concentration. More importantly, it was found that terameprocol **2**, NDGA derivative **3** and NDGA derivative

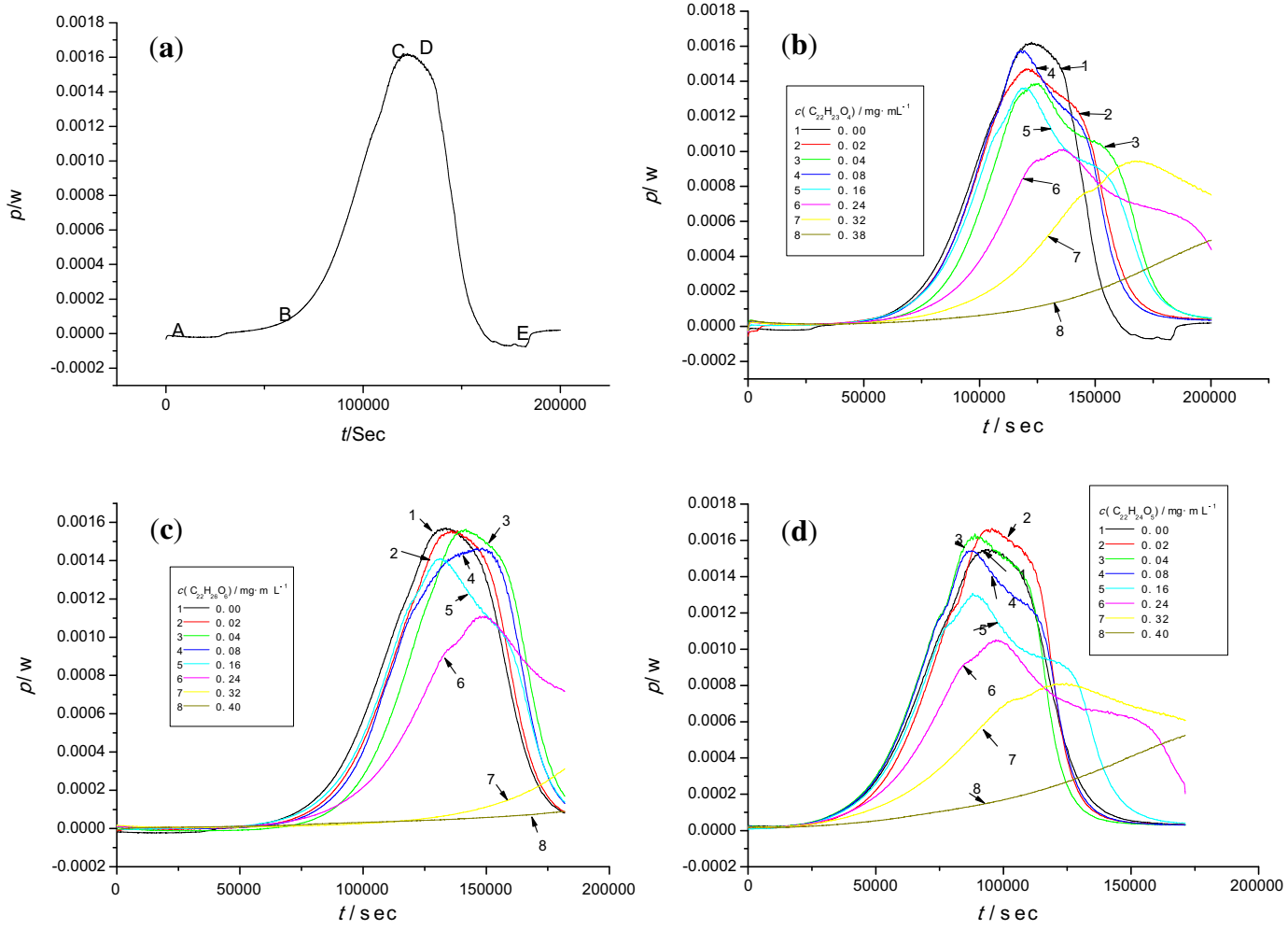

Fig. 4. Metabolism thermogenic curves of *S. pombe* cells affected by the compounds at 32.00 °C. (a): For control; (b): For terameprocol **2**; (c): For NDGA derivative **3**; (d): For NDGA derivative **4**.

Table 1
Thermokinetic parameters of the growth of *S. pombe* affected by inhibitors at different concentrations at 32.00 °C.

Inhibitors	c^a/mg·L^{-1}	k^b/min^{-1}	R^c	I^d	IC_{50}^e/mg·L^{-1}
Terameprocol **2**	0.00	$0.00443 \pm 3.7723 \times 10^{-6}$[f]	0.9987	0.00	330.0
	20.00	$0.00401 \pm 2.391 \times 10^{-6}$	0.9995	9.48	
	40.00	$0.00407 \pm 2.7923 \times 10^{-6}$	0.9991	8.13	
	80.00	$0.00425 \pm 2.1328 \times 10^{-6}$	0.9995	4.06	
	160.0	$0.00392 \pm 1.4008 \times 10^{-6}$	0.9997	11.51	
	240.0	$0.00322 \pm 1.2102 \times 10^{-6}$	0.9997	27.31	
	320.0	$0.00245 \pm 1.2343 \times 10^{-6}$	0.9993	44.70	
	380.0	$0.00143 \pm 4.8528 \times 10^{-7}$	0.9997	67.72	
NDGA derivative **3**	0.00	$0.00444 \pm 4.7937 \times 10^{-6}$	0.9980	0.00	290.0
	20.00	$0.00479 \pm 5.1510 \times 10^{-6}$	0.9980	−7.88	
	40.00	$0.00462 \pm 6.3506 \times 10^{-6}$	0.9973	−4.05	
	80.00	$0.00460 \pm 4.7560 \times 10^{-6}$	0.9977	−3.60	
	160.0	$0.00421 \pm 3.0529 \times 10^{-6}$	0.9988	5.18	
	240.0	$0.00341 \pm 2.0422 \times 10^{-6}$	0.9991	23.20	
	320.0	$0.00163 \pm 8.4427 \times 10^{-7}$	0.9991	63.29	
	400.0	$0.00075 \pm 3.6659 \times 10^{-7}$	0.9990	83.00	
NDGA derivative **4**	0.00	$0.00422 \pm 1.3357 \times 10^{-6}$	0.9998	0.00	350.0
	20.00	$0.00427 \pm 1.7166 \times 10^{-6}$	0.9996	−1.18	
	40.00	$0.00429 \pm 1.8595 \times 10^{-6}$	0.9996	−1.66	
	80.00	$0.00431 \pm 2.1920 \times 10^{-6}$	0.9994	−2.13	
	160.0	$0.00430 \pm 2.3583 \times 10^{-6}$	0.9994	−1.90	
	240.0	$0.00346 \pm 2.1549 \times 10^{-6}$	0.9991	18.00	
	320.0	$0.00273 \pm 2.7096 \times 10^{-6}$	0.9983	35.31	
	400.0	$0.00113 \pm 5.7325 \times 10^{-6}$	0.9990	73.22	

[a] The concentration.
[b] The growth rate constant of *K562*.
[c] The correlation coefficient.
[d] The inhibitive ratio.
[e] The half inhibition concentration.
[f] Mean ± S.D.; $n = 3$.

4 possessed better inhibitory activities on the growth metabolism of *K562* than *S. pombe* cell lines. That is because the values of IC_{50} of terameprocol **2**, NDGA derivative **3** and NDGA derivative **4** on the growth metabolism of *K562* cell lines were found to be 5.87, 8.57 and 11.23 mg L^{-1}, respectively, which is much smaller than those of terameprocol **2**, NDGA derivative **3** and NDGA derivative **4** on the growth metabolism of *S. pombe* cell lines. The inhibitory ability of these three compounds above on the growth of *K562* has been

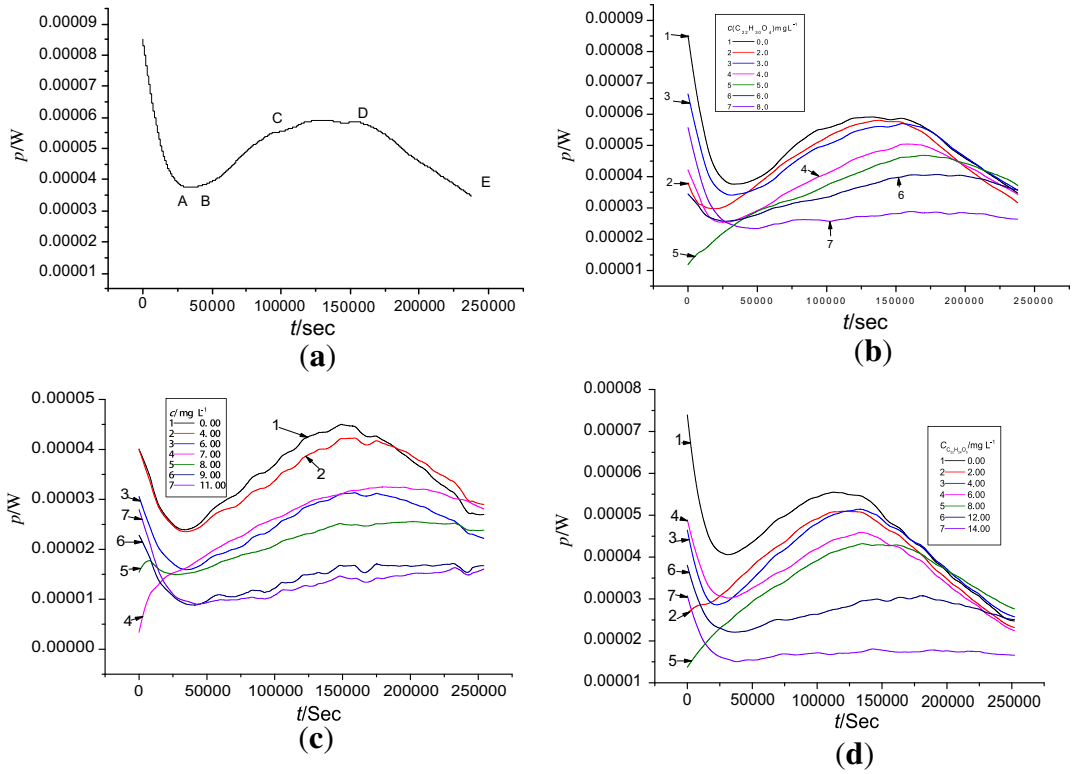

Fig. 5. Metabolism thermogenic curves of *K562* cells affected by the compounds at 37.00 °C. (a): For control; (b): For terameprocol **2**; (c): For NDGA derivative **3**; (d): For NDGA derivative **4**.

Table 2
Thermokinetic parameters of the growth of *K562* affected by inhibitors at different concentrations at 37.00 °C.

Inhibitors	c^a/mg L^{-1}	k^b/min^{-1}	R^c	I^d	$IC_{50}{}^e$/mg L^{-1}
Terameprocol **2**	0.00	$4.1881 \times 10^{-4} \pm 1.00210 \times 10^{-6}$[f]	0.9932	0.00	5.87
	2.00	$4.7239 \times 10^{-4} \pm 7.1697 \times 10^{-7}$	0.9952	−12.79	
	3.00	$4.4342 \times 10^{-4} \pm 7.5337 \times 10^{-7}$	0.9954	−5.88	
	4.00	$3.9762 \times 10^{-4} \pm 6.0102 \times 10^{-7}$	0.9961	5.06	
	5.00	$2.7992 \times 10^{-4} \pm 3.0152 \times 10^{-7}$	0.9967	33.16	
	6.00	$1.9712 \times 10^{-4} \pm 3.2544 \times 10^{-7}$	0.9934	52.93	
	8.00	$8.5275 \times 10^{-5} \pm 4.3549 \times 10^{-7}$	0.9375	79.64	
NDGA derivative **3**	0.00	$3.9397 \times 10^{-4} \pm 7.3096 \times 10^{-7}$	0.9911	0.00	8.57
	4.00	$4.4893 \times 10^{-4} \pm 4.9357 \times 10^{-7}$	0.9945	−13.95	
	6.00	$3.9703 \times 10^{-4} \pm 7.2831 \times 10^{-7}$	0.9922	−0.78	
	7.00	$3.6261 \times 10^{-4} \pm 9.4969 \times 10^{-7}$	0.9948	7.96	
	8.00	$2.2866 \times 10^{-4} \pm 4.9898 \times 10^{-7}$	0.9953	41.96	
	9.00	$1.7435 \times 10^{-4} \pm 8.4754 \times 10^{-6}$	0.8884	55.75	
	11.00	$1.6810 \times 10^{-4} \pm 5.3231 \times 10^{-7}$	0.9442	57.33	
NDGA derivative **4**	0.00	$3.8465 \times 10^{-4} \pm 7.4564 \times 10^{-7}$	0.9946	0.00	11.23
	2.00	$3.9155 \times 10^{-4} \pm 3.7194 \times 10^{-7}$	0.9941	−1.79	
	4.00	$4.3527 \times 10^{-4} \pm 8.7860 \times 10^{-7}$	0.9938	−13.16	
	6.00	$3.1202 \times 10^{-4} \pm 4.4618 \times 10^{-7}$	0.9972	18.88	
	8.00	$3.0855 \times 10^{-4} \pm 4.9220 \times 10^{-7}$	0.9959	19.78	
	12.00	$1.6500 \times 10^{-4} \pm 4.4866 \times 10^{-7}$	0.9806	57.10	
	14.00	$7.6784 \times 10^{-5} \pm 5.8538 \times 10^{-7}$	0.8605	80.04	

[a] The concentration.
[b] The growth rate constant of *K562*.
[c] The correlation coefficient.
[d] The inhibitive ratio.
[e] The half inhibition concentration.
[f] Mean ± S.D.; $n = 3$.

observed to decrease in the order of terameprocol **2** > NDGA derivative **3** > NDGA derivative **4**.

2.2.2. Pharmacological mechanisms

The results of the stained *K562* cells were illustrated in Fig. 6. The experimental results showed that cells of control group, i.e. normal cells without any drugs inhibition (Fig. 6a) were round, varied in size and had some big spherical protrusions and a small amount number of microvilli on the surface. At the same time, there existed some notches on their nuclear surface. In addition, intracytoplasmic mitochondrial showed some small tubes with thick crest and abundant free mitochondrial ribosomes. After *K562* cells were treated by the terameprocol **2** (Fig. 6b), it was found that the cell membrane structure changed. It was further found that, the nuclear size became smaller, the chromatin gathered under nuclear envelope, and the nuclear membrane structure was clear. Moreover, cell membrane structure showed early apoptotic, and necrosis and rupture of membrane happened in partial cell. Cell membrane structure disappeared, and cytoplasm filled by a large number of lipid droplets. Cell surface extended long protrusions. All of these observations confirmed that there were late apoptotic changes in cell membrane structure. Furthermore, the treated cells stained using PI (propidium iodide) (Fig. 6c) showed that the cell nucleus changed red, which demonstrated the late apoptotic changes.

The results of mitochondrial transmembrane potential of *K562* cells were shown in Table 3.

The above experimental results showed that the mitochondrial transmembrane potential of *K562* cells treated by drugs decreased significantly comparing with the control group. The potentials of high concentration groups were smaller than those of low concentration groups, and were found to be decreased significantly as time went on. The difference between groups had statistical significance by *t*-test.

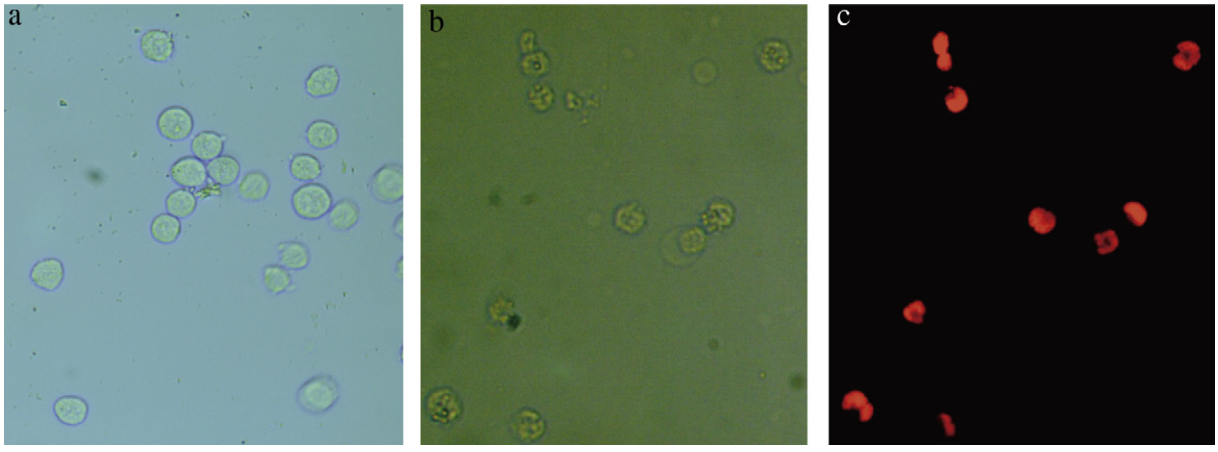

Fig. 6. Morphological change of *K562* cells: (a) Control group; (b) treated by terameprocol **2**; (c) the PI staining of the cells treated by terameprocol **2**.

Table 3
Mitochondrial transmembrane potential of *K562* cells affected by terameprocol **2** at different concentrations ($\bar{x} \pm s$, $n = 3$).

Drug concentration mg/L	R h123(%)		
	12 h	18 h	24 h
Control	668.2 ± 0.8	788.8 ± 1.0	277.9 ± 1.4
4.0	597.2 ± 0.6	615.3 ± 1.5[a]	168.0 ± 2.3[a]
6.0	477.8 ± 2.8[a]	331.5 ± 2.9[a]	170.7 ± 1.2[a]

[a] Compared with control group $p < 0.01$.

Mitochondria are one of the most important organelles for cells. It is well known that mitochondria are apoptosis receptors and amplifier of cell survival in many physiological or pathological situations. Thus, mitochondria play a very important role in cell survival [14]. The permeability transition pores of mitochondria located in the junction of outer and inner membranes of mitochondria, which is formed by a variety of protein components. It is because of the opening of the permeability transition pores that a series of phenomenon such as the decrease or disappearance of the potential of the mitochondrial membrane, the swelling of mitochondrial, the rupturing of outer membrane, the activation of caspases, and the releasing of cytochrome occurred. It is indicated that mitochondria participated in the apoptosis of cells and some important events in the apoptotic cascade [15].

3. Conclusions

In this paper, we report the synthesis and characterization of terameprocol **2**, NDGA derivative **3** and its cyclized analogue **4**. Their bioactivities on *S. pombe* and *K562* cell lines have been also determined by microcalorimetry. The preliminary results showed that the values of IC_{50} of terameprocol **2**, NDGA derivative **3** and NDGA derivative **4** on the growth metabolism of *S. pombe* cell lines were 330.0, 290.0 and 350.0 mg L^{-1}, respectively; the values of IC_{50} of terameprocol **2**, NDGA derivative **3** and NDGA derivative **4** on the growth metabolism of *K562* cell lines were 5.87, 8.57 and 11.23 mg L^{-1}, respectively. The inhibitory activity of these compounds on the growth of the *S. pombe* has been observed to decrease in the order of NDGA derivative **3** > terameprocol **2** > NDGA derivative **4**. While their inhibitory activity on *K562* cell lines was found to decrease according to the order: terameprocol **2** > NDGA derivative **3** > NDGA derivative **4.** The compounds **2, 3** and **4** possessed the bidirectional biological effect and Hormesis effect. They stimulated the growth of the *S. pombe* and *K562* at low concentration, but inhibited the growth of *S. pombe* and *K562* at high concentration.

The experimental has substantiated elementarily that terameprocol **2** possessed the action of inducing cancer cell-apoptosis, reducing mRNA levels and subsequent protein production of the cyclin-dependent kinase CDC2, resulting in the inactivation of the CDC2/cyclin B complex (maturation promoting factor) [16]. The antitumor activities of terameprocol **2** may be based on selective inhibition of specificity protein 1 (Sp1)-regulated proteins, including VEGF, survivin and cdc2 that control cell cycle and apoptosis [17–19].

4. Experiments

4.1. Synthesis

4.1.1. 3,4-Dimethoxypropiophenone (*7*)

This compound was prepared by a modified procedure based on the method of Perry et al. [10] as outlined in Fig. 3. To a 5 L, 4-necked round bottom flask (equipped with N_2 inlet, overhead magnetic stir drive, addition funnel, thermocouple, and condenser) was added aluminum chloride (349 g, 2.61 mol) followed by CH_2Cl_2 (870 mL). The suspension was cooled to −10 °C using a dry ice/acetone bath. Propionyl chloride (138 g, 1.49 mol) in CH_2Cl_2 (145 mL) was added in portions via addition funnel over 15 min. Keeping the mixture between −2 °C and 2 °C, the mixture was stirred for an additional 10 min. Veratrole (170 g, 1.23 mol) in CH_2Cl_2 (100 mL) was added via the addition funnel over 20 min, the reaction mixture was kept under the temperature between −4 °C and 1 °C. After 5 min, TLC showed complete consumption of starting material (SiO_2, 1:1 EtOAc–heptane, UV, veratrole $R_f = 0.54$, propiophenone $R_f = 0.42$). The reaction was cooled to −10 °C and hydrochloric acid (3 M, 2 L) was slowly and cautiously added over 25 min while keeping the reaction mixture between −1 °C and 16 °C. The phases were separated and the aqueous phase was extracted once with CH_2Cl_2 (500 mL). The combined CH_2Cl_2 was washed with NaOH (3 M, 1 L), dried over $MgSO_4$ (34.5 g), and then concentrated *in vacuo* to give a viscous oil. The oil was dissolved in hot MeOH (300 mL) and the solution was held at 0–5 °C for 16 h. The resulting white solids were broken up with spatula and vacuum filtered. The filter cake was washed with heptane (125 mL) and dried on the funnel (179.9 g). A second crop of solids was obtained by concentrating the mother liquor, diluting with MeOH and holding at 0–5 °C for 3 h (15 g). The crop 1 and 2 solids were combined and dried in a vacuum oven (30 °C, 18 h) to give propiophenone **7** as a white solid (192 g, 80.5% yield, purity >98% as determined by HPLC). ^{1}H NMR ($CDCl_3$, 400 MHz) δ: 1.21 (*t*, 3H, $J = 7.3$ Hz), 2.96 (q, 2H, $J = 7.3$ Hz), 3.93 (s, 3H), 3.94 (s, 3H), 6.88 (d, 1H, $J = 8.3$ Hz), 7.54 (d, 1H, $J = 1.6$ Hz), 7.58 (dd, 1H, $J = 8.3$, 1.6 Hz). ^{13}C NMR ($CDCl_3$, 100 MHz) δ: 8.27, 30.98, 55.64, 55.73, 109.74, 109.83, 122.24, 129.87, 148.69, 152.79, 199.10. LC/MS ($m/z = 194.8$).

4.1.2. 2-Bromo-3,4-dimethoxypropiophenone (*8*)

This compound was prepared by a modified procedure based on the method of Perry et al. [10], as outlined in Fig. 3. A 3 L, 3-neck round bottom flask was fitted with an addition funnel, overhead magnetic stir, thermocouple, N_2 inlet and condenser. The condenser was vented into a base trap containing NaOH (50.2 g, 1.26 mol) in 1.8 L deionized water. The vessel was charged with propiophenone **7** (241.55 g, 1.25 mol) and chloroform (900 mL). The mixture was heated to 62–64 °C. To the refluxing solution was added a solution of bromine (203.9 g, 1.27 mol, in 300 mL chloroform) via the addition funnel over 35 min. The reaction mixture was vigorously stirring during addition. After addition, the mixture was vigorously stirred for 20 min and cooled to 20 °C. The solvent was removed *in vacuo* and the resulting solids were dissolved in $CHCl_3$ (250 mL) and MeOH (625 mL). The solution was concentrated until solids formed and the slurry was cooled to 0–5 °C hand held for 10 min. The slurry was vacuum filtered on a 2 L fritted funnel (medium frit), and the filter cake was washed with cold MeOH (2 × 50 mL). The solids were dried in a vacuum oven (35 °C, 15 h) to give 228 g α-bromoketone **8** (67% yield). A second crop was obtained by concentrating the mother liquor to a solid, and crystallizing from hot MeOH (300 mL) to give an additional 58 g α-bromoketone **8** (17.3% yield). ^{1}H NMR ($CDCl_3$, 400 MHz) δ: 1.90 (d, 3H, $J = 6.7$ Hz), 3.95 (s, 3H), 3.96 (s, 3H), 5.29 (q, 1H, $J = 6.7$ Hz), 6.91 (d, 1H, $J = 8.4$ Hz), 7.59 (d, 1H, $J = 2.0$ Hz), 7.66 (dd, 1H, $J = 8.4$, $J = 2.0$ Hz). ^{13}C NMR ($CDCl_3$, 100 MHz) δ: 20.23, 41.13, 55.90, 109.96, 111.03, 123.35, 126.85, 149.10, 153.69, 191.94. LC/MS ($m/z = 274.8$).

4.1.3. 1,4-Bis(3,4-dimethoxyphenyl)-2,3-dimethylbutane-1,4-dione (*3*)

As outlined in Fig. 3, to a dry 5 L, 3-necked round bottom flask (equipped with an overhead magnetic stir drive, addition funnel, thermocouple and N_2 inlet and outlet) was added solid 97% *t*-BuOK

(103 g, 898.5 mmol, corrected for purity), followed by THF (615 mL). The solution was cooled to 0–1 °C with an ice-water bath. A solution of propiophenone **7** (170 g, 876.3 mmol) in THF (340 mL) was added in portions over 15 min while keeping the internal temperature <7 °C giving a white/yellow-white slurry. After 15 min the mixture was warmed to 18 °C and DMF (850 mL) was added via the addition funnel over 2 min giving a clear yellow/orange solution. After 15 min, the reaction mixture was cooled to −70 °C using a dry ice/acetone bath. With vigorous stirring, a solution of α-bromoketone **8** (240 g, 876.3 mmol) in 2:1 THF-DMF (510 mL) was added in portions over 25 min while maintaining an internal temperature between −60 °C and −55 °C. After an additional 15 min at −60 °C, the reaction was complete as determined by LC/MS analysis. The reaction was quenched at −60 °C with water (900 mL) containing 70 mL 1 M HCl and the reaction was warmed to 18–20 °C over 1 h. The bulk of THF was removed *in vacuo* (1415 mL solvent removed) and the resulting mixture was extracted with CH_2Cl_2 (1.5 L). The organic layer was separated and the aqueous layer (pH 2–3) was back extracted twice with CH_2Cl_2 (2 × 400 mL). The combined CH_2Cl_2 was washed with water (425 mL). The bulk of the CH_2Cl_2 (1550 mL) was removed *in vacuo* to give crude product **3**, which was further purified from methanol to give the expected product 321.7 g (95% yield, purity>98% as determined by HPLC). ^{1}H NMR ($CDCl_3$, 400 MHz) δ: 1.31 (d, J = 7.1 Hz, $2CH_3$, 6H), 3.55 (m, 2H), 3.85 (s, $4OCH_3$, 12H), 6.98 (d, 2H, J = 6.9 Hz), 7.24–719 (m, 4H). ^{13}C NMR ($CDCl_3$, 100 MHz) δ: 11.82, 42.11, 58.87, 110.14, 110.23, 131.33, 149.44, 150.11, 198.22. LC/MS (m/z = 386.4).

4.1.4. 2,5-Bis(3,4-dimethoxyphenyl)-3,4-dimethylfuran (**4**)

To a dry 50 L, 3-necked round bottom flask (equipped with a mechanical stirrer, addition funnel, thermocouple and N_2 inlet and outlet) was added solid 97% *t*-BuOK (774.8 g, 6.56 mol, corrected for purity), followed by THF (4.60 L). The solution was cooled to 0–4 °C with an ice-water bath. A solution of propiophenone **7** (1.243 kg, 6.40 mol) in THF (2.50 L) was added in portions over 60 min while keeping the internal temperature <7 °C giving a white/yellow-white slurry. After 15 min the mixture was warmed to 10 °C and DMF (6.20 L) was added via the addition funnel over 15 min giving a clear yellow/orange solution. After 15 min, the reaction mixture was cooled to −70 °C using a dry ice/acetone bath. With vigorous stirring, a solution of α-bromoketone **8** (1.748 kg, 6.4 mol) in a solution of 2:1 THF-DMF (THF: 2.5 L; DMF: 1.25 L) was added in portions over 90 min while maintaining an internal temperature between −60 °C and −55 °C. After an additional 15 min at −60 °C, the reaction was complete as determined by LC/MS analysis. The reaction was quenched at −60 °C with water (8.60 L) containing 1M HCl 510 mL and the reaction were warmed to 18–20 °C over 1 h. The bulk of THF was removed *in vacuo* (9000 mL solvent removed) and the resulting mixture was extracted with CH_2Cl_2 (5.6 L). The organic layer was separated and the aqueous layer (pH 2–3) was back extracted twice with CH_2Cl_2 (2 × 7.6 L). The combined CH_2Cl_2 was washed with water (3.5 L). The bulk of the CH_2Cl_2 (8000 mL) was removed *in vacuo* and was transferred to a 3-neck round bottom flask equipped with mechanical stirrer, addition funnel and condenser. The resulting solution was heated to reflux (44 °C) and a solution of 3% HCl in MeOH (prepared by adding 460 mL acetyl chloride to 8000 mL methanol) was added in a steady stream over a period of 90 min. Solids precipitated within 15–20 min. Reflux was continued (54 °C) for 5 h and the mixture was cooled to 0–2 °C over 2 h. The solids were vacuum filtered and the filter cake was washed with MeOH (2920 mL), then heptane (2920 mL). The white solids were dried in a vacuum oven (20 h, 50 °C), then the solid was stirred and crushed to break down larger pieces. The solid was dried in a vacuum oven (20 h, 50 °C). The procedure was repeated 3 times till solid was completely dried (no weight loss between drying turns), which gave 2194 g of furan **4** (91% yield, purity>98% as determined by HPLC). ^{1}H NMR ($CDCl_3$, 400 MHz) δ: 2.22 (s, 6H), 3.92 (s, 6H), 3.95 (s, 6H), 6.94 (d, 2H, J = 6.9 Hz), 7.24–719 (m, 4H). ^{13}C NMR ($CDCl_3$, 100 MHz) δ: 9.82, 55.87, 55.90, 109.14, 111.25, 117.77, 118.36, 125.06, 146.86, 148.00, 148.92. LC/MS (m/z = 368.8).

4.1.5. Terameprocol (**2**)

Terameprocol **2** is anticancer drug candidate currently in clinical trials. Large quantity of terameprocol **2** may be needed in the future. We were interested in exploring synthetic process which would allow us to effectively produce terameprocol **2** at kilograms per batch since methods reported in the literature [10] was not scalable in our hand. By using different catalysts, solvents, reaction temperatures, reaction times, and hydrogen pressures, we were able to develop three optimized procedures (methods A, B and C), which were scalable, reproducible and could produce terameprocol **2** at relatively large quantity.

4.1.5.1. Method A. To an 8 L hydrogenator, equipped with an overhead magnetic stir drive and heating mantle, were charged a finely divided mixture of 78.65 g (32.6 mmol) 10% Pd-C catalyst (10R39, 55.9% wet) catalyst (available through Johnson–Matthey Inc) and 11.55 g (5.4 mmol) Degussa E101 10% Pd/C (50% wet) catalyst (available from Sigma–Aldrich Inc.). To the vessel was charged *n*-propyl acetate (3.74 L) and the vessel was pressurized to 800 psi with H_2. The mixture was stirred at the maximum stir speed at room temperature for 30 min to 1 h. The vessel was vented to atmospheric pressure, the lid opened under N_2 atmosphere and slurry of furan compound **4** (400 g, 108 mmol) in *n*-propyl acetate (1.86 L was charged to the vessel). The mixture was heated to 100 °C under 1000 psi H_2 pressure at maximum stir speed. The reaction was monitored by HPLC until all furan **4** is consumed and less than 2% THF intermediate **9** is present. The reaction mixture was cooled to 20–25 °C and the vessel was vented to atmospheric pressure. The reactor lid was removed and the reaction mixture was sparged with N_2. Immediately, the reaction mixture was filtered through a bed of Celite® 545 filter material (800 g) and the Celite® filter material cake was washed with *n*-propyl acetate (4 L). The combined *n*-propyl acetate filtrate was washed with water (2 L), 5 wt % aqueous potassium carbonate solution (2 L) and brine (2 L). The organic stream was dried over Na_2SO_4 (400 g), filtered, and then solvent was removed *in vacuo* at 50 °C. The resulting residue was diluted with heptane (2 L) and solvent was removed *in vacuo* at 50 °C. The resulting solids were suspended in 15% (v/v) IPA–heptane (1.6 L), heated to 50–60 °C and cooled to 20 °C over 1 h. The slurry was agitated for 1 h at 20 °C and vacuum filter (up to 18 h). The crude solids were transferred (289 g) to a 2 L vessel, equipped with an overhead stir drive, condenser and heating mantle, and 15% (v/v) IPA–heptane (578 mL) was added. The mixture was heated to 65 °C until the slurry thinned (about 5 min) and the mixture was allowed to cool to 15 °C over 3.5 h. The slurry was vacuumed and the cake was washed with chilled (5–10 °C) 15% (v/v) IPA–heptane (300 mL). The solids were dried *in vacuo* to constant weight (217 g, 55.9% yield, purity > 99% as determined by GC). ^{1}H NMR ($CDCl_3$, 400 MHz) δ: 0.85 (d, 6H, J = 6.6 Hz), 1.83–1.92 (m, 2H), 2.30 (dd, 2H, J = 9.3, 13.5 Hz), 2.76 (dd, 2H, J = 5.0, 13.5 Hz), 3.85 (s, 6H), 3.86 (s, 6H), 6.65 (d, 2H, J = 2.0 Hz), 6.70 (dd, 2H, J = 8.0, 2.0 Hz), 6.79 (d, 2H, J = 8.0 Hz). ^{13}C NMR ($CDCl_3$, 200 MHz) δ: 16.19, 38.80, 39.14, 55.76, 55.86, 110.99, 112.22, 120.90, 134.42, 147.02, 148.68. LCMS (m/z = 358.9).

4.1.5.2. Method B. Furan compound **4** (400 g) was hydrogenated in *n*-propyl acetate using 10R39 catalyst (2.5 mol%) and E101 NE/W GG (0.5 mol%) at 100 °C. After pre-reducing the catalyst mixture at

Table 4
Results of hydrogenation of furan **4** under various pressure and time.

No.	Time (h)	T (°C)	P (psi)	Furan **4** (%)	Compound **9** (%)	Terameprocol **2** (%)	Other impurity (%)
1	1	100	960	NA	NA	NA	NA
2	2	100	980	18.2	29.5	38.4	13.9
3	3	100	980	0.0	24.7	55.4	19.9
4	4	100	980	0.0	17.1	61.2	21.7
5	5	100	980	0.0	11.8	64.7	23.5
6	6–18	23	980–600	Held without stirring, water added at $t = 18$ h			
7	18	23	600	0.0	9.5	64.1	26.4
8	21	100	950	0.0	4.3	67.9	27.8
9	22	100	840	0.0	2.8	67.1	30.1
10	Isolated product (46.6% yield)			0.0	1.2	98.2	0.6

room temperature, the reactor lid was opened and substrate was added as a solid. The mixture was heated under H_2 pressure and monitored by HPLC. The reaction scheme is shown in Fig. 3 and the reaction profile is shown in Table 4. Within 3 h, the furan **4** was completely converted to THF intermediate **9** and products (Table 4, entry 3). The amount of THF intermediate **9** steadily decreased over the next 2 h (Table 4, entries 4–5), and the mixture was cooled to room temperature and held for 12 h (Table 4, entry 6). Water (10% by volume of *n*-PrOAc) was then added and the mixture was heated under H_2 pressure. After an additional 4 h of heating under H_2 pressure, HPLC analysis showed low levels of THF intermediate **9** (Table 4, entry 9).

After filtering the mixture through Celite® filter material and washing the filter cake with additional *n*-propyl acetate, the product stream underwent aqueous work-up. The solvent was evaporated and the residual *n*-propyl acetate was chased with heptane. Terameprocol was then crystallized from heptane. The resulting sticky solids were difficult to manipulate and a spatula was used to free the solids from the walls of the vessel. After filtration, three heptane washes were used to remove the residual cyclized impurity 48 from terameprocol. After drying *in vacuo* at 50 °C, terameprocol was isolated in 46.6% yield, with 98.2% purity (by HPLC) (Table 4, entry 10). Analytical data were identical with that shown in Method A.

4.1.5.3. Method C. In this reaction, several modifications based on the results in entries 6–9 were implemented in order to optimize the yield and purity of terameprocol **2**. First, to avoid a slower conversion, consistent H_2 pressure was maintained at 1000 psi during the reaction. Second, to improve conversion of starting material to products, the loading of 10R39 catalyst was increased from 2.5 mol% to 3 mol%. Third, in order to avoid unnecessary losses due to either product absorption onto carbon or decomposition under acidic conditions, the reaction mixture was filtered through Celite® filter material immediately upon reaction completion. Finally, to avoid losses during product isolation the product was initially isolated from 15% IPA–heptane, then reslurried with IPA–heptane instead of washing several times with heptane.

After pre-reducing the catalyst, the vessel was opened and a slurry of the furan compound **4** (400 g) in *n*-propyl acetate was added. The mixture was heated and the pressure was carefully monitored to ensure consistent pressure (1000 psi) during the course of the reaction. The results for this run, using 3.0 mol% 10R39 catalyst and 0.5 mol% Degussa E101 catalyst, monitored by HPLC, are shown in Table 5. After 3 h, complete consumption of furan **4** was observed by HPLC (Table 5, entry 1). Within the next 5 h, the THF intermediate **9** was steadily converted to products (Table 5, entries 2–4). After 8 h, the reaction mixture was cooled to room temperature and immediately filtered through Celite® filter material. The organic stream was held overnight at room temperature.

After the overnight hold, the organic stream was concentrated under vacuum till dryness to give waxy solids, which were then slurried in 15% IPA–heptane (4 mL/g input) at 55 °C for 15 min and the resulting uniform slurry was cooled to 20 °C over 1 h. After an additional 1 h of stirring at 20 °C, the slurry was filtered. Instead of immediately washing the cake with heptane, the cake was allowed to dry on the vacuum funnel. The resulting crude cake (289.58 g), was transferred to a vessel (2 L) and suspended in 15% IPA–heptane (2 mL/g). The suspension was heated to 65 °C and held until the slurry thinned (5 min). The slurry was cooled to 15 °C over 4 h, vacuum filtered, then washed once with chilled 15% IPA–heptane (1 mL/g, cooled to 5–10 °C). After drying *in vacuo* at 70 °C, terameprocol was isolated in 55.9% yield, with 99.0% purity (by HPLC). Analytical data were identical with that shown in Method A.

4.2. Determination of bioactivity

4.2.1. Cell lines and culture conditions

S. pombe (ACCC 20047) was provided by Agricultural Culture Collection of China. The Edinburgh minimal medium (YES) culture composition was 5 g/L yeast extract, 30 g/L glucose, 225 mg/L adenine, histidine, leucine, uracil and lysine hydrochloride. The yeast extract medium composition was dissolved by 100 mL distilled water and constant volume to 1000 mL (natural pH).

K562 (3115CNCB00237) was provided by China Center for Type Culture Collection. The complete growth medium: RPMI 1640 medium with 2 mM L-glutamine adjusted to contain 1.5 g/L sodium bicarbonate, 4.5 g/L glucose, 10 mM HEPES and 1.0 mM sodium pyruvate 90%, fetal bovine serum 10%, 100 μg/mL streptomycin, 100 μg/mL Penicillin.

Table 5
Results of hydrogenation of furan **4** under various reaction times.

No.	Time (h)	T (°C)	P (psi)	Furan **4** (%)	Compound **9** (%)	Terameprocol **2** (%)	Other impurity (%)
1	3	100	1000	0.0	21.4	58.5	20.1
2	5	100	1000	0.0	5.6	69.1	25.3
3	7	100	1000	0.0	2.8	70.2	26.9
4	8	100	1000	0.0	1.2	70.6	28.2
5	Isolated product (55.9% yield)			0.0	0.0	99.0	0.5

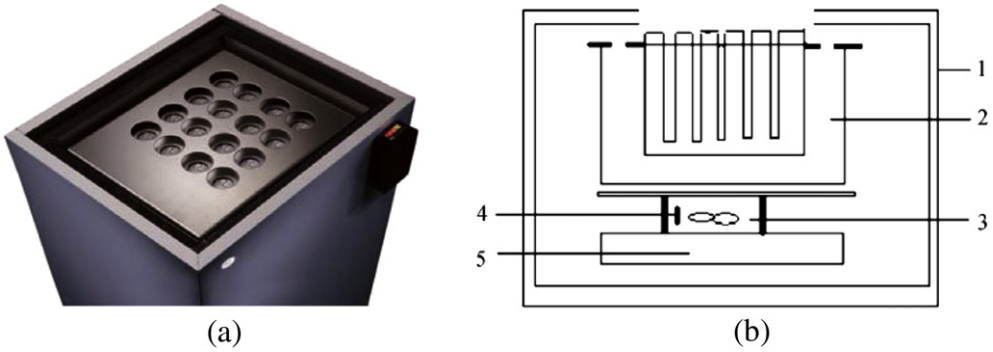

Fig. 7. TAM air isothermal calorimeter. (a) The outside drawing. (b) The schematic diagram. 1: Air thermostat; 2: calorimeter unit; 3: fan; 4: temperature sensor; 5: Peltier temperature control module.

4.2.2. Microcalorimeter

An eight-channel heat conduction isothermal microcalorimeter (Fig. 7, 3116-2/3239 TAM air, Thermometric AB Company, Sweden) was employed in this research. This eight-channel heat conduction isothermal microcalorimeter for heat flow measurements in the milliwatt range under isothermal conditions was held together in a single removable block. The block was placed in an air thermostat, which kept the temperature within 0.02 °C indicating that temperature gradient is very low. All calorimetric channels were of twin type, consisting of a sample and a reference vessel. Each vessel was connected to the surrounding heat sink by a Peltier module, and when heat was produced or consumed due to any process, the temperature of the sample vessel was to be changed. The temperature of the surrounding was constant and thus a temperature gradient across the Peltier module was developed. This would generate a measurable voltage and the voltage was proportional to the heat flow across the Peltier module and to the rate of the processes taking place in the sample vessel. Such voltage signal was recorded continuously and in real-time through an eight channel data acquisition system connected to a computer. The software supplied to TAM air was used to monitor and record the heat flow over the Peltier module when the baseline drift was less than 20 μW over 24 h.

The microcalorimetric measurements of *S. pombe* and *K562* were carried out on a TAM air isothermal microcalorimeter at 32.00 °C and 37.00 °C, respectively. Baselines were taken before each measurement and the calorimeter was calibrated electrically. More details of the performance of the instrument are available in the literature [20]. When the system had gained a stable baseline, 5 mL sterilized culture medium was added into the sterilized sample ampoules. *S. pombe* and *K562* were inoculated with an initial density of 1×10^6 cells mL^{-1}. Samples of three compounds at different concentrations were added to the cell suspension, respectively. All the microcalorimetric experiments were repeated three times and the results were identical.

4.2.3. Cytomorphology and fluorescence probe method

To investigate the action mechanism of the terameprocol on *K562* cells, here we divided *K562* cells into 3 groups: control group (0 mg/L), low-dose group (4.0 mg/L) and high-dose group (6.0 mg/L). *K562* cells in each group were incubated for 12, 18 and 24 h at 37 °C in a 5% CO_2 atmosphere, respectively. And then 1 mL *K562* cells were collected from each group, they were washed three times with PBS and added Propidium Iodide (PI) (Sigma–aldrich Co.), then incubated for 5 min in the dark. The dye was washed with PBS. Images were obtained via an inverted fluorescence microscope (DSZ5000X China). At the same time, 1 mL *K562* cells were collected from each group, they were washed three times with PBS and added Rhodamine (Rh123) (Sigma–Aldrich Co.), then incubated for 45 min in the dark. The dye was washed with PBS. Mitochondrial transmembrane potentials were assessed using a fluorescence spectrophotometer (F-4600 Hitachi Co., Japan) [21]. Date are given as mean ± S.D. at least 3 individual experiments. The results were analyzed by *t*-test using SPSS 19.0 software.

Acknowledgments

This research was financially supported by the National Natural Science Foundation of China (No. 20973145 and No. 21273190), the Hunan Provincial Key Laboratory Special Foundation of China (No. 2011TP4016-1), the Hunan Provincial Educational Ministry Foundation of China (No. 11A112), and the Construct Program of the Key Discipline in Hunan Province. Prof. Qiang-Guo Li (E-mail: liqiangguo@163.com) is the chief-director of these fund projects.

References

[1] Q. Chen, Curr. Top. Med. Chem. 9 (2009) 1636–1659.
[2] S. Arteaga, A. Andrade-Cetto, R. Cárdenas, J. Ethnopharmacol. 98 (2005) 231–239.
[3] J. Craigo, M. Callahan, R.C.C. Huang, A.L. DeLucia, Antivir. Res. 47 (2000) 19–28.
[4] J.M. Lu, J. Nurko, S. Weakley, J. Jiang, P. Kougias, P. Lin, Q. Yao, C. Chen, Med. Sci. Monitor 16 (2010) RA93–100.
[5] M.L.C. Montanari, A.E. Beezer, C.A. Montanari, D. Piló-Veloso, J. Med. Chem. 43 (2000) 3448–3452.
[6] Q. Li, H. Zhang, X. Li, B. Wang, J. Hu, F. Yao, D. Yang, S. Xiao, L. Ye, Chin. J. Chem. 29 (2011) 2285–2292.
[7] X. Li, Q.G. Li, H. Zhang, J.L. Hu, F.H. Yao, D.J. Yang, S.X. Xiao, L.J. Ye, Y. Huang, D.C. Guo, Biol. Trace Elem. Res. 147 (2012) 366–373.
[8] D. Zhang, Y. Liu, Y. Zhang, X.J. Chen, Y.F. Shen, Environ. Toxicol. Pharmacol. 22 (2006) 121–127.
[9] W. Kong, J. Wang, X. Xing, X. Xiao, Y. Zhao, Q. Zang, P. Zhang, C. Jin, Z. Li, W. Liu, Anal. Chim. Acta 689 (2011) 250–256.
[10] C.W. Perry, M.V. Kalnins, K.H. Deitcher, J. Org. Chem. 37 (1972) 4371–4376.
[11] C.W. Perry, US 3906004, 1975.
[12] H.M. Faid Allah, R. Soliman, J. Heterocycl. Chem. 24 (1987) 667–671.
[13] J.C.G. Cortés, E. Carnero, J. Ishiguro, Y. Sánchez, A. Durán, J.C. Ribas, J. Cell. Sci. 118 (2005) 157–174.
[14] G. Lenaz, Biochim. Biophys. Acta 1366 (1998) 53–67.
[15] D.A. Hildeman, T. Mitchell, T.K. Teague, P. Henson, B.J. Day, J. Kappler, P.C. Marrack, Immunity 10 (1999) 735–744.
[16] C.C. Chang, J.D. Heller, J. Kuo, R.C.C. Huang, S. Roseman, Proc. Natl. Acad. Sci. USA 101 (2004) 13239–13244.
[17] D.E. Hansel, S. Dhara, R.C. Huang, R. Ashfaq, M. Deasel, Y. Shimada, H.S. Bernstein, J. Harmon, M. Brock, A. Forastiere, M.K. Washington, A. Maitra, E. Montgomery, Am. J. Surg. Pathol. 29 (2005) 390–399.
[18] J.D. Lambert, R.O. Meyers, B.N. Timmermann, R.T. Dorr, Cancer Lett. 171 (2001) 47–56.
[19] R. Park, C.C. Chang, Y.C. Liang, Y. Chung, R.A. Henry, E. Lin, D.E. Mold, R.C.C. Huang, Clin. Cancer Res. 11 (2005) 4601–4609.
[20] Q.G. Li, D.J. Yang, X. Li, L.J. Ye, D.L. Wei, S.X. Xiao, Acta Chim. Sin. 66 (2008) 2686–2692.
[21] T. Mosmann, J. Immunol. Methods 65 (1983) 55–63.